

# EXTRACTING PRINTED DESIGNS AND WOVEN PATTERNS FROM TEXTILE IMAGES

Wei Jia, Stephen J. McKenna and Annette A. Ward  
*School of Computing, University of Dundee, Dundee, Scotland, U.K.*

**Keywords:** Textile segmentation, Pixel labelling, Markov random field, Quantitative evaluation.

**Abstract:** The extraction of printed designs and woven patterns from textiles is formulated as a pixel labelling problem. Algorithms based on Markov random field (MRF) optimisation and reestimation are described and evaluated on images from an historical fabric archive. A method for quantitative evaluation is presented and used to compare the performance of MRF models optimised using  $\alpha$ -expansion and iterated conditional modes, both with and without parameter reestimation. Results are promising for potential application to content-based indexing and browsing.

## 1 INTRODUCTION

Accurate automatic extraction of printed designs and woven patterns from images of textiles is an important task in providing a suitable representation on which to build algorithms for the retrieval and browsing of digital textile archives. This paper discusses colour segmentation of digital images in a historical commercial archive owned by Liberty Fabric, the fabric design division of Liberty, London's iconic department store. The Liberty digital archive consists of many thousands of images, primarily comprising textile swatches from the past century. Some designs are printed on the surface of the fabric and other designs are formed as part of the weave of the fabric. Although many of the images are from the previous 50 years, there are many that are much older, are only fragments, or have degraded over time; thus adding complexity to the problem of extraction.

In general the problem of image segmentation is ill-defined with more than one reasonable segmentation solution for a given image. Furthermore, many textile and art images consist of abstract patterns that make segmentation more challenging. Figure 1(a) shows a 6-colour design with sketchy flowers and Figure 1(b) illustrates one possible manual segmentation of that design into different design components (i.e., flowers and leaves).

Formulation of the problem of segmentation of printed designs and woven patterns requires consideration of textile production. There are various methods

of textile coloration and production. Contemporary production of Liberty Fabric prints require making a screen for each colour used in a design. This can be done by hand tracing or by computer reduction and separation. Dye is applied to the fabric by flat screens for short runs and rotary screens for long runs and continuous designs. However, not all designs in the archive are printed. Some designs are woven into the fabric through the weaving process that may be simple, in the case of stripes, or more complex; for example, jacquard.

Figure 1(c-g) shows a ground truth for the original image in Figure 1(a) that was obtained by manually assigning its pixels to one of five classes (i.e., colours). However, in a large database, manual labeling is not feasible. Thus, the problem to be solved is to determine the number of classes in a digital textile image and label each pixel as belonging to one of these classes. Solutions to this problem can be quantitatively evaluated by comparing computer extractions with manually-annotated ground-truths such as those shown in Figure 1(c-g).

Another aspect that may complicate the problem of segmenting a digital image into colour regions is the physical surface texture of the fabric (Figure 2). This is affected by the fibres (e.g., smooth or crimped), yarns (e.g., soft or hard twist; number of plies), fabric construction (e.g., type of weave or knit), and/or textile finishing (e.g., brushing or chemical application). All of these factors may impact the visual texture of the image. Methods based on clus-

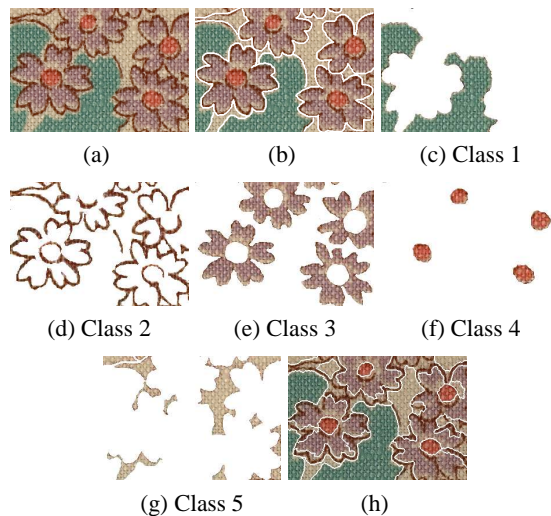


Figure 1: (a) A textile image (©Liberty Fabric). (b) One of many reasonable (manual) segmentations. (c-g) A manually obtained class labeling of the pixels (h) A JSEG segmentation.

tering pixels in a colour space without considering the spatial coherence of the clusters will fail in such cases. Further difficulties arise due to the age and condition of the textiles, especially in historic archives. For printed textiles, the saturation of a dye varying within a region (either due to degradation or by design) may be problematic. Printing may result in screens being misaligned and in dyes blending together near their boundaries to form new colours. However, these effects are sometimes deliberately introduced to create additional colour variation or to help ensure that the fabric is entirely covered with dye leaving no undyed areas.

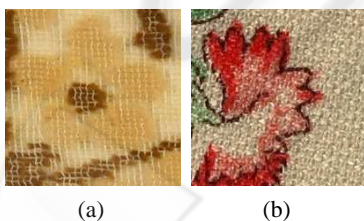


Figure 2: (a) The underlying fabric can be strongly textured. (b) Colour dyes can blend together and have spatially-varying density (Images ©Liberty Fabric).

Markov random field (MRF) models have been used previously for image segmentation, though usually for binary foreground-background segmentation tasks. In this paper, an MRF model is formulated and applied to the textile segmentation task described above. Given ground-truth estimates of colour separation, this application provides a useful test case

for comparing algorithms. A method for quantitative evaluation of multi-class pixel labelling methods is proposed that handles segmentations with different numbers of labels. It is used to compare segmentation results obtained by Gaussian mixture colour clustering, MRF inference using Iterated Conditional Modes (ICM), and MRF inference using  $\alpha$ -expansion. The MRF models consider both the class colour distributions and the spatial coherence of the pixel labels. The colour distributions are initialised based on a labelling estimated using a Gaussian mixture in colour space. The number of colour classes is estimated using the Bayes Information Criterion (BIC).

Some related work is described in Section 2. The MRF model along with the algorithms selected to perform learning and inference are described in Section 3. Section 4 describes the evaluation method and Section 5 reports comparative results obtained using this method. Finally, Section 6 draws some conclusions and mentions some plans for future work.

## 2 RELATED WORK

Clustering of local image features or pixel values is often performed using K-means clustering or Gaussian mixture model (GMM) parameter estimation with Expectation-Maximisation (EM) (e.g. (Gupta and Sortrakul, 1998; Wu et al., 2003; Permuter et al., 2003)). Such clustering treats the features or pixel values as independent and so when used for segmentation the results often lack spatial coherence, especially when the images exhibit strong texture. Images of fabric have been segmented using colour clustering after first attenuating noise and texture by applying median filtering (Valiente et al., 2001). However, the use of a median filter as a preprocessing step can result in important details being lost. The JSEG segmentation algorithm (Deng and Manjunath, 2001) performs colour clustering at the pixel level and then uses region growing on the cluster labels to segment colour-texture regions. An example JSEG result is shown in Figure 1(h)<sup>1</sup>. Whilst JSEG can find reasonable colour-texture regions, it has two drawbacks. Firstly, it decomposes the task into two steps of colour clustering and region finding so that the colour clustering step takes no account of spatial information. Secondly, fabric designs have spatially disjoint regions that share the same colour-texture. We seek a labelling that makes this explicit.

<sup>1</sup>The JSEG implementation of Deng and Manjunath was used with default parameters. See <http://vision.ece.ucsb.edu/segmentation/jseg/>

Markov random field (MRF) can provide spatial constraints in a neighborhood system in the image domain. They have been used to perform spatially coherent pixel clustering and promising qualitative results were reported on two outdoor scenes (Zabih and Kolmogorov, 2004). Kato and Pong reported some quantitative segmentation results using an MRF with pixel colour and local texture features (Kato and Pong, 2006). However, they assumed that the number of labels was known. Furthermore, the MRF energy optimisation methods used by Kato and Pong no longer represent the state of the art. Comparative studies of MRF optimisation methods on various computer vision problems have shown methods based on graph cuts to be effective (Boykov et al., 2001; Szeliski et al., 2008).

### 3 MRF SEGMENTATION

Each pixel  $p$  is to be assigned a label  $f_p$  which takes a value from a discrete label set  $\{1, \dots, K\}$  with  $f$  denoting a particular labelling of all the pixels. The purpose is to obtain the labelling  $\hat{f}$  that is most probable given the image  $x$ ,

$$\hat{f} = \operatorname{argmax}[P(f|x)] = \operatorname{argmax}[P(x|f)P(f)] \quad (1)$$

According to the Hammersley-Clifford theorem (Li, 1995), the prior probability of a particular labelling is:

$$P(f) \propto \exp\left(-\sum_C V_C(f_p, f_q)\right) \quad (2)$$

where the sum is over all cliques in a neighborhood system and  $V_C$  is a clique potential. A clique is defined as a subset of pixels in the neighborhood system. The MRFs used in this paper consider adjacent pixel locations to be neighbours (4-connectivity) and the clique potentials involve pairs of pixels, so formulation (2) becomes:

$$P(f) \propto \exp\left(-\sum_p \sum_{q \in N_p} V(f_p, f_q)\right) \quad (3)$$

where  $q$  is the neighborhood of  $p$ . An important discontinuity preserving metric function is given by the Potts model (Potts, 1952):

$$V(f_p, f_q) = \lambda \cdot (1 - \delta(f_p - f_q)) \quad (4)$$

If labels  $p$  and  $q$  are different ( $f_p \neq f_q$ ), then its value is  $\lambda$ . Otherwise its value is zero.

Note that the pixel features are assumed independent given the labels, so

$$P(x|f) = \prod_p P(x_p|f_p) \quad (5)$$

The likelihood of a label,  $f_p$ , given its pixel,  $x_p$ , is modelled as Gaussian,

$$P(x_p|f_p = k) = \frac{\exp\left[-\frac{1}{2}(x_p - \mu_k)^T \Sigma_k^{-1} (x_p - \mu_k)\right]}{\sqrt{(2\pi)^d |\Sigma_k|}} \quad (6)$$

with parameter set  $\theta_k$  which consists of the mean,  $\mu_k$ , and the covariance matrix,  $\Sigma_k$ .

Thus, the problem of segmenting an image is formulated as labelling each pixel with one of  $K$  possible labels and is achieved by minimizing the following energy function.

$$E(f) = \sum_p \sum_{q \in N_p} \lambda \cdot (1 - \delta(f_p - f_q)) - \sum_p \ln(P(x_p|f_p)) \quad (7)$$

where the constant  $\lambda \geq 0$  is a coefficient that specifies the penalty for assigning different labels to neighboring pixels. Eq. (7) has two terms: the first is a smoothing term that rewards spatial coherence and the second is a data term.

#### 3.1 Energy Function Minimisation

The energy minimisation problem can be solved by using the  $\alpha$ -expansion algorithm (Szeliski et al., 2008). The variable  $\alpha$  takes values in  $\{1, 2, \dots, K\}$  iteratively. Within one  $\alpha$ -expansion, some of the labels are simultaneously changed to  $\alpha$  while all others remain unchanged. This gives a new labelling  $f$  which is accepted only if it reduces the energy. In general there are an exponential number of possible expansion moves. A graph-based min-cut/max-flow algorithm (Boykov and Kolmogorov, 2004) has been used to find the optimal expansion move, namely to find the lowest energy within one  $\alpha$ -expansion. The  $\alpha$ -expansion algorithm is guaranteed to converge, terminating when there is no energy decrease for all values of  $\alpha$ .

An alternative and older method, iterated conditional modes (ICM) (Besag, 1986), uses a greedy strategy to find a local minimum of the energy function. For each pixel in turn, the algorithm chooses the label which results in the lowest energy. This is repeated until convergence. ICM has been reported to be very sensitive to the initialisation of the labelling.

##### 3.1.1 Initialisation

The number of labels,  $K$ , and the initial labelling, are both estimated using a GMM to model the pixel values in RGB space. Bayes' Information Criterion (BIC) has been found by various authors to give reasonable results when selecting the number of components in a Gaussian mixture, e.g. (Roberts et al.,

1998). Given maximum likelihood parameter estimates  $\hat{\theta}$ , the number of the components is selected as

$$K_{BIC} = \underset{K}{\operatorname{argmin}} \left\{ -L(X|\hat{\theta}, K) + \frac{1}{2}M(K) \ln N \right\} \quad (8)$$

where  $L(X|\hat{\theta})$  is the log likelihood,  $N$  is the number of samples, and  $M(K)$  is the number of free parameters in the model which in the case of a 3-D GMM with full covariance matrices is  $M(K) = (1/2)Kd^2 + (3/2)Kd + K - 1$ , where  $d=3$ . Given the initial labelling, the parameters of the class-conditional Gaussians (Eq. 6) are estimated from the pixel data classified as belonging to that class (using MAP classification).

### 3.1.2 Parameter Re-Estimation

A useful strategy is to alternate energy reduction and parameter estimation in a manner similar to Expectation-Maximisation. In the ‘‘E’’ step, the Gaussian parameters are fixed and a new labeling is found. Given the new labelling, the parameters of the Gaussians are re-estimated conditioned on this labelling (the ‘‘M’’ step). This results in a new energy function, the value of which the next ‘‘E’’ step should reduce. Since parameter estimation is relatively fast, it seems reasonable in the case of  $\alpha$ -expansion to re-estimate the Gaussian parameters after each new expansion step (Zabih and Kolmogorov, 2004).

## 4 EVALUATION METHOD

Ground-truth labelling can be produced for each image by manual annotation. For visualisation, these labels are mapped to contrasting colours. The accuracy of an automated labelling is then evaluated by comparing it to the ground-truth. However, the label values are interchangeable. Furthermore, the labelling obtained will not generally have the same number of label values as the ground-truth. If two segmentations use  $N$  and  $M$  labels respectively then there are  $R(M, N) = \frac{M!}{(M-N)!}$  ( $0 < N \leq M$ ) possible mappings between the  $N$  labels in one segmentation and the  $M$  labels in the other segmentation. Note that  $U = M - N$  labels will not find a match ( $U \geq 0$ ). The measure of segmentation error which we use is the percentage of pixels labelled differently from the ground-truth in the mapping that minimises this percentage, i.e.,

$$\mathcal{E} = \min_{\Pi} \frac{100}{m} \sum_{p=1}^m \delta(f_p^{(1)} - \Pi(f_p^{(2)})) \quad (9)$$

where  $f_p^{(1)}$  and  $f_p^{(2)}$  are labels assigned to the same pixel in the two segmentations, and  $\Pi$  denotes a permutation of the labels. Note that labels that do not find a match will contribute to this error. The percentage of pixels with unmatched labels will be denoted  $\mathcal{U}$ .

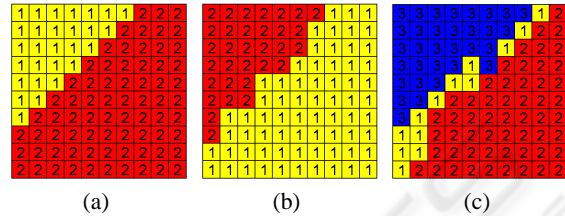


Figure 3: (a) A ground-truth labelling of a  $10 \times 10$  pixel image. (b-c) Two automatically produced labellings.

Figure 3 shows a simple example for the purposes of illustration. There are  $R(2, 2) = 2$  possible permutations between Figure 3(a) and Figure 3(b):  $\begin{pmatrix} 1 & \rightarrow & 1 \\ 2 & \rightarrow & 2 \end{pmatrix}$  and  $\begin{pmatrix} 1 & \rightarrow & 2 \\ 2 & \rightarrow & 1 \end{pmatrix}$  where  $a \rightarrow b$  means label value ‘‘a’’ in labelling 1 corresponds to label value ‘‘b’’ in labelling 2. Clearly, the latter produces a lower error. It is this error which is reported. In the same way, there are  $R(3, 2) = 6$  possible permutations between Figure 3(a) and Figure 3(c). The permutation that results in the lowest error is:  $\begin{pmatrix} 1 & \rightarrow & 3 \\ 2 & \rightarrow & 2 \\ & & 1 \end{pmatrix}$ . In this case, labels with value ‘‘1’’ in labelling 2 are unassigned and so contribute to the error. The accuracy of the labelling in Figure 3(c) is thus  $\mathcal{E} = 17\%$  of which  $\mathcal{U} = 13\%$  is attributable to unmatched labels resulting from incorrect estimation of the number of labels,  $K$ .

## 5 RESULTS AND DISCUSSION

Methods were quantitatively evaluated on images from a commercial textile archive. The images ranged in size from  $200 \times 200$  pixels to  $2648 \times 1372$  pixels. These images present challenges to segmentation algorithms as discussed in Introduction. Ground-truth labellings were produced manually. The test program was implemented in C and ran on an Intel Core 2 Quad Q6600 2.40GHz PC.

Five methods were evaluated. The first method was Gaussian mixture model clustering using maximum likelihood EM parameter estimation. Each pixel was labelled with the most probable Gaussian component index conditioned on the pixel’s RGB values. The second and third methods were MRF labellings

found using ICM with and without parameter reestimation, denoted ICM and ICM(P) respectively. The fourth and fifth methods were MRF labellings found using  $\alpha$ -expansion with and without parameter reestimation, denoted  $\alpha$  and  $\alpha$ (P) respectively. The free parameter in the MRF models was set to  $\lambda=6$  (see Eq.(7)) for all images.

Table 1 reports results when the number of labels was assumed known (i.e.,  $K$  was the same as in the ground-truth). Table 2 reports results for the more difficult (and more realistic) situation in which  $K$  was unknown. The value of  $K$  was estimated based on the BIC values obtained when EM was used to optimise the parameters of the GMM. The number of colour dyes used is often limited by production costs in the type of textile production represented in the data set. Therefore, very large values of  $K$  can be ruled out *a priori*. Specifically, values of  $K$  from 1 to 10 were considered.

Tables 1 and 2 show the errors evaluated using the method in Section 4 as well as the execution times. The images, their ground-truth, and segmentations are shown in Tables 3 to 7. In every case,  $\alpha$ -expansion with parameter estimation gave the lowest error. In many cases ICM with parameter estimation performed better than  $\alpha$ -expansion without parameter estimation. This suggests that parameter reestimation is important for these methods. GMM gave the highest error. In every case,  $\alpha$ -expansion with parameter reestimation was the slowest. ICM(P) was slower than ICM,  $\alpha$ (P) was slower than  $\alpha$  and GMM was fastest. For each algorithm, computational expense increases with  $K$ .

Printing was not always used to create the textiles. In the textile image in Table 3, there are four different colours of filling yarn (i.e., the yarn that runs horizontally). However, the strong texture and uneven appearance resulted in BIC estimating  $K$  as 7. The graph plots the BIC value against  $K$ . Error bars denote  $\pm$  a standard deviation ( $\sigma$ ) estimated over 10 runs for each value of  $K$ . Segmentation results using  $K = 4$  and  $K_{BIC} = 7$  are shown. In both cases,  $\alpha$ -expansion with parameter reestimation is clearly superior.

It is interesting to note that although  $K$  was usually overestimated by BIC, the effect of this on the segmentation error for  $\alpha$ -expansion with parameter reestimation was not always large. For example, it can be seen that there is no large difference in error with different  $K$  in Table 3. The  $\alpha$ -expansion algorithm can be understood as a competition between different labels. In every expansion,  $\alpha$  takes one value from  $\{1, 2, \dots, K\}$  and makes some of the pixels become  $\alpha$  simultaneously. If the change is accepted, parameters will be reestimated, a learning process. This helps

to balance the percentage of different labels. The ground-truth for the textile image in Table 3 contains four colours, while  $K_{BIC} = 7$ , but after  $\alpha$ -expansion with re-estimation only 0.4% of pixels are assigned labels 5, 6, or 7. Similar comments apply to the textile images in Table 5 and Table 6. Sometimes, larger  $K$  can help to distinguish similar colors. For example, in Table 6,  $K = 8$  is not enough to distinguish the brown and red colors due to the texture effects and dye degradation, but  $K_{BIC} = 9$  could and gave a smaller error rate.

In the fabric in Table 7, filling yarns were inserted into the warp yarns to create the floral pattern. Here, when  $K = 3$ ,  $\alpha$ (P) is superior to the other methods, but when  $K_{BIC} = 7$ , although  $\alpha$ (P) is better than others, it loses accuracy.

Tables 4 and 5 show less strongly-textured fabrics. Nevertheless, they are problematic. A small cropped patch of the textile image in Table 5 is shown magnified in Figure 4(b) where yellow and blue regions overlap and create green. In order to avoid gaps between different colour regions, two dyes may be overlapped slightly, thus producing a third colour and causing difficulty for colour segmentation. Figure 4 graphically illustrates this problem. Figure 4(c) shows an annotated ground-truth. However, the  $\alpha$ -expansion method separates the overlapping area into another colour region as shown in Figure 4(d).

## 6 CONCLUSIONS

In this paper, we have addressed colour separation of textiles in order to recover printed designs and woven patterns from archival image data. An evaluation method was proposed and used to compare pixel labellings obtained using MRFs optimised using  $\alpha$ -expansion and ICM both with and without parameter reestimation. These algorithms were initialised based on Gaussian mixture colour models and BIC was used to select the number of distinct class labels.

For all the images tested,  $\alpha$ -expansion with parameter reestimation was the most accurate and the most computationally expensive method.  $\alpha$ -expansion without parameter reestimation gave similar performance to ICM with parameter reestimation. BIC based on GMM usually overestimated the number of class labels. However, this did not always result in  $\alpha$ -expansion with parameter reestimation obtaining a less accurate result. In fact, in one case the accuracy was improved.

The pixel labellings produced suggest ways of compactly representing image content in terms of colour and shape. Future work will explore their use

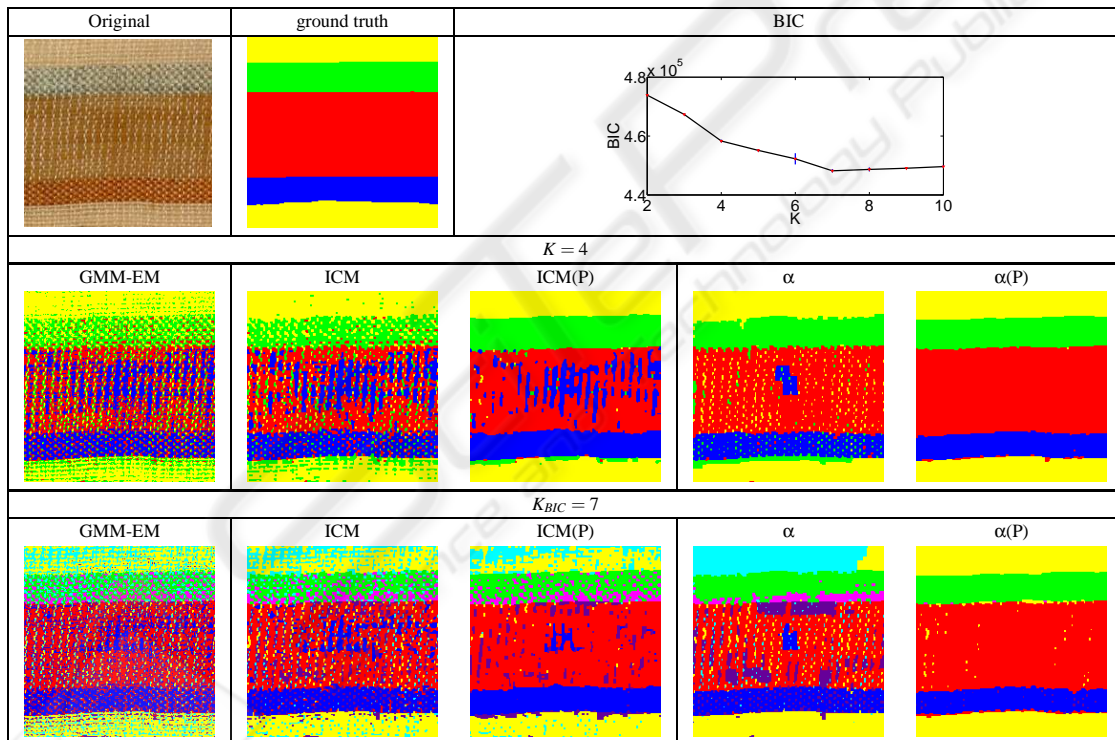
Table 1: Error rates and computing times with known  $K$ .

Image			Error(%): $\varepsilon$					Time (s)				
Table	Size	K	GMM	ICM	ICM(P)	$\alpha$	$\alpha(P)$	GMM	ICM	ICM(P)	$\alpha$	$\alpha(P)$
3	200×200	4	39.07	30.85	13.56	11.68	3.30	0.19	0.36	1.14	0.93	1.21
4	1400×544	7	20.85	17.40	15.90	17.04	12.83	7.70	12.93	39.40	50.53	53.76
5	1268×556	7	17.05	14.27	12.23	12.90	6.63	7.02	11.82	36.21	34.21	65.95
6	996×608	8	48.99	42.89	31.56	34.18	24.99	4.97	9.61	33.49	29.11	50.82
7	1594×896	3	25.60	24.00	22.67	23.39	4.65	5.20	10.18	33.09	36.62	55.01

Table 2: Error rates and computing times with  $K$  estimated automatically.

Image		Error(%): $\varepsilon$ [ $\sigma$ ]					Time (s)				
Table	$K_{BIC}$	GMM	ICM	ICM(P)	$\alpha$	$\alpha(P)$	GMM	ICM	ICM(P)	$\alpha$	$\alpha(P)$
3	7	44.97[30.39]	35.00[25.25]	19.99[17.07]	32.75[27.65]	5.52[0.40]	0.28	0.55	1.87	1.19	2.53
4	7	20.85[0.00]	17.40[0.00]	15.90[0.00]	17.04[0.00]	12.83[0.00]	7.70	12.93	39.40	50.53	53.76
5	9	18.31[9.69]	16.12[9.58]	15.05[9.53]	15.39[9.54]	8.37[4.43]	9.11	15.03	46.13	53.16	100.10
6	9	47.79[6.83]	40.75[5.64]	30.623[9.19]	34.66[8.32]	19.01[0.50]	7.96	12.88	39.49	34.47	63.02
7	7	45.15[44.10]	42.99[42.34]	45.27[44.92]	46.76[46.37]	37.53[36.76]	10.52	20.40	70.44	115.41	190.27

Table 3: Segmentation results on a 200×200 textile image (©Liberty Fabric).



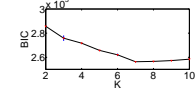
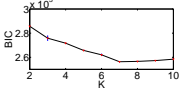
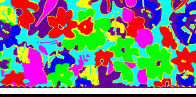
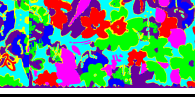
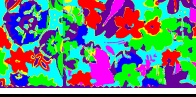
in content-based retrieval and browsing.

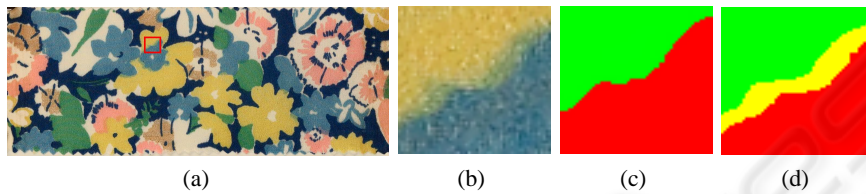
## ACKNOWLEDGEMENTS

The authors wish to thank Anna Buruma and Martin Coward of Liberty Fabric, and Peter Taylor for helpful discussions and advice. This research was supported by the UK Technology Strategy Board grant

“FABRIC: Fashion and Apparel Browsing for Inspirational Content” in collaboration with Liberty Fabric, System Simulation, Calico Jack Ltd., and the Victoria and Albert Museum. The Technology Strategy Board is a business-led executive non-departmental public body, established by the government. Its mission is to promote and support research into, and development and exploitation of, technology and innovation for the benefit of UK business, in order to in-

Table 4: Segmentation results on a  $1400 \times 544$  textile image (©Liberty Fabric).

Original	Ground truth	BIC		
				
$K = K_{BIC} = 7$				
GMM-EM	ICM	ICM(P)	$\alpha$	$\alpha(P)$
				

Figure 4: (a) Cropping a small patch of original image (b) Original image patch (c) “Ground truth” (d)  $\alpha$ -expansion result.

crease economic growth and improve the quality of life. It is sponsored by the Department for Innovation, Universities and Skills (DIUS). Please visit: <http://www.innovateuk.org/> for further information.

## REFERENCES

- Besag, J. (1986). On the statistical analysis of dirty pictures. *Journal of Royal Statistical Society, Series B*, 48(3):259–302.
- Boykov, Y. and Kolmogorov, V. (2004). An experimental comparison of min-cut / max-flow algorithms for energy minimization in vision. *IEEE Transactions on Pattern Analysis and Machine Intelligence*, 26:1124–1137.
- Boykov, Y., Veksler, O., and Zabih, R. (November 2001). Fast approximate energy minimization via graph cut. *IEEE Transactions on Pattern Analysis and Machine Intelligence*, 23, no. 11:1222–1239.
- Deng, Y. and Manjunath, B. (2001). Unsupervised segmentation of color-texture regions in images and video. *IEEE Transactions on Pattern Analysis and Machine Intelligence*, 23:800–810.
- Gupta, L. and Sortrakul, T. (1998). A Gaussian mixture based image segmentation algorithm. *Pattern Recognition*, 31(3):315–325.
- Kato, Z. and Pong, T. C. (2006). A Markov random field image segmentation model for color texture images. *Image and Vision Computing*, 24:1103–1114.
- Li, S. Z. (1995). *Markov Random Field Modeling in Computer Vision*. Springer-Verlag.
- Permuter, H., Francos, J., and Jermyn, I. H. (2003). Gaussian mixture models of texture and color for image database retrieval. *Acoustics, Speech and Signal Processing*, 3:569–572.
- Potts, R. (1952). Some generalized order-disorder transformation. *Proc. Cambridge Philosophical Soc.*, 48:106–109.
- Roberts, S. J., Husmeier, D., Rezek, I., and Penny, W. (1998). Bayesian approaches to Gaussian mixture modeling. *IEEE Transactions on Pattern Analysis and Machine Intelligence*, 20(11):1133–1142.
- Szeliski, R., Zabih, R., Scharstein, D., Veksler, O., Kolmogorov, V., Agarwala, A., Tappen, M., and Rother, C. (2008). A comparative study of energy minimization methods for Markov random fields with smoothness-based priors. *IEEE Transactions on Pattern Analysis and Machine Intelligence*, 30:1068–1080.
- Valiente, J. M., Carretero, M. C., Gmis, J. M., and Albert, F. (2001). Image processing tool for the purpose of textile fabric modeling. In *12th International Conference on Design Tools and Methods*.
- Wu, Y., Yang, X., and Chan, K. L. (2003). Unsupervised colour image segmentation based on Gaussian mixture model. *Information, Communications and Signal Processing*, 1:541–544.
- Zabih, R. and Kolmogorov, V. (2004). Spatially coherent clustering using graph cuts. *IEEE Computer Society Conference on Computer Vision and Pattern Recognition*, 2:473–444.

Table 5: Segmentation results on a  $1268 \times 556$  textile image (©Liberty Fabric) with small texture affection.

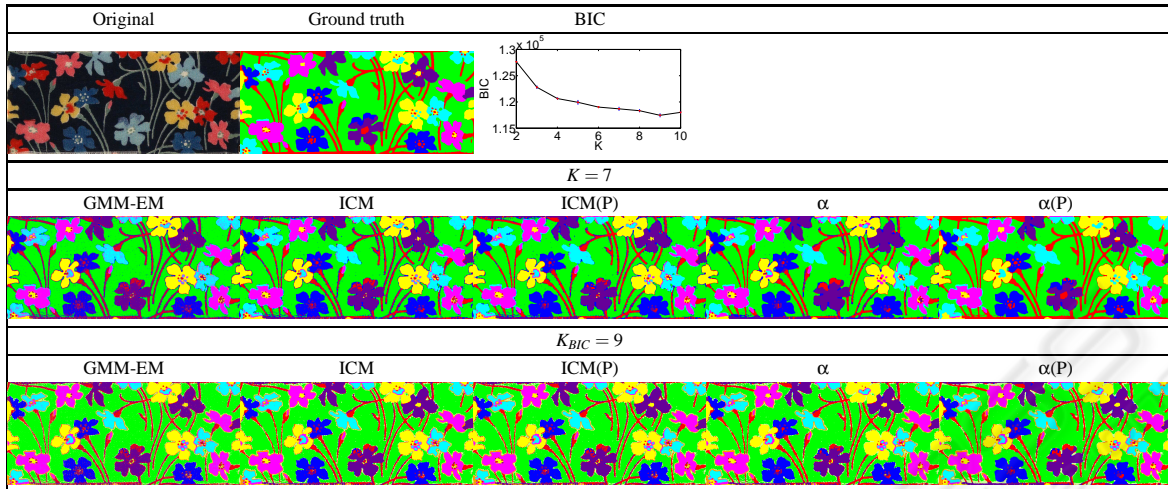


Table 6: Segmentation results on a  $996 \times 608$  textile image (©Liberty Fabric).

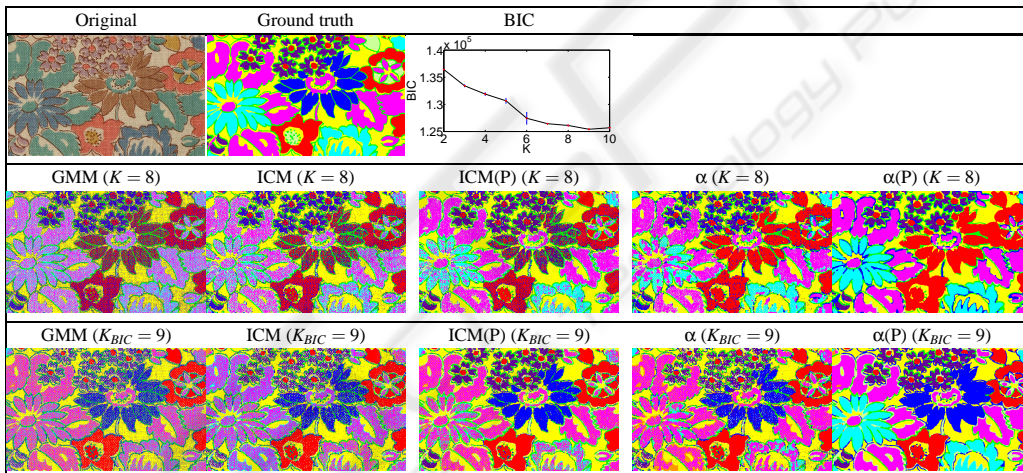


Table 7: Segmentation results on a  $1594 \times 896$  textile image (©Liberty Fabric).

